



HAL
open science

3D Printing and Physical Modeling of Musical Instruments: Casting the Net

Romain Michon, Chris Chafe, John Granzow

► **To cite this version:**

Romain Michon, Chris Chafe, John Granzow. 3D Printing and Physical Modeling of Musical Instruments: Casting the Net. Sound and Music Computing Conference, 2018, Limassol, Cyprus. hal-02159009

HAL Id: hal-02159009

<https://hal.science/hal-02159009>

Submitted on 18 Jun 2019

HAL is a multi-disciplinary open access archive for the deposit and dissemination of scientific research documents, whether they are published or not. The documents may come from teaching and research institutions in France or abroad, or from public or private research centers.

L'archive ouverte pluridisciplinaire **HAL**, est destinée au dépôt et à la diffusion de documents scientifiques de niveau recherche, publiés ou non, émanant des établissements d'enseignement et de recherche français ou étrangers, des laboratoires publics ou privés.

3D Printing and Physical Modeling of Musical Instruments: Casting the Net

Romain Michon^{†*} and Chris Chafe[†]

[†]CCRMA, Stanford University (USA)

*GRAME, Lyon (France)

rmichon@ccrma.stanford.edu

John Granzow

School of Music, Theater, and Dance

University of Michigan, Ann Arbor (USA)

jgranzow@umich.edu

ABSTRACT

Predicting the acoustics of objects from computational models is of interest to instrument designers who increasingly use Computer Assisted Design. We examine techniques to carry out these estimates using a database of impulse responses from 3D printed models and a custom algorithm for mode interpolation within a geometrical matrix. Test geometries are organized as a function of their physical characteristics and placed into a multidimensional space/matrix whose boundaries are defined by the objects at each corner. Finite Element Analyses is integrated into the open-source CAD environment to provide estimates of material vibrations also compared to measurements on the fabricated counterparts. Finally, predicted parameters inform physical models for aural comparisons between fabricated targets and computational estimates. These hybrid methods are reliable for predicting early modes as they covary with changes in scale and shape in our test matrix.

1. INTRODUCTION

In the last decade we have seen numerous attempts to use 3D printing to produce musical instruments [1–3]. Print resolution increases, material limitations are overcome, and machine costs have come down for entry level printers, dissolving barriers for modern luthiers interested in such techniques. The use of Computer Assisted Design (CAD) softwares such as SolidWorks,¹ Rhino,² OpenScad,³ etc. is a necessary step in the digital fabrication process.⁴ Musical instruments must therefore be modeled first on a computer before being printed.

We believe that physical/acoustical modeling has an important role to play in this context by allowing luthiers to listen to a digital version of their instrument before materializing it. Additionally, 3D printing presents a unique opportunity to test existing physical modeling techniques in a

¹<http://www.solidworks.com/> (All the URLs presented in this paper were verified on March 6, 2018)

²<https://www.rhino3d.com/>

³<http://www.openscad.org/>

⁴Error prone 3D scanning may be used to derive geometries from pre-existing objects, however modifying these meshes for novel designs requires much more expensive software.

highly controlled environment where the physical properties (e.g., material, shape, etc.) of the objects to be modeled can be precisely controlled.

The idea of using physical modeling to tune the characteristics of musical instruments before making them is not new and has been investigated in the framework of various projects [4,5], but absent from these earlier efforts was the ability of the maker to listen to a virtual version of the instrument when prototyping it on a computer.

Physical modeling of musical instruments has made significant progress in recent years and realistic virtual versions of existing instruments can be implemented. However, each instrument presents different challenges and there doesn't exist a lightweight generic solution to model any instrument from knowledge of its geometry and materials that can be represented in a CAD model.

In this paper, we investigate the use of various techniques to predict and approximate the sound of an object before printing it. We focus on simplified string instrument bodies/resonators to facilitate comparisons between the printed objects and their virtual version.

Rather than an exhaustive approach, we focus on simple techniques wary of how emerging challenges would increase with more complex instruments.

First, we present the 3D printed objects used for our experiments. Next, we analyze their impulse response by extracting modal information from them. We then compare the modal profiles computed with the Finite Element Method (FEM) on their 3D models to the measurements from their physical counterparts. After this, we introduce a new modeling method using mode morphing on a database of impulse response and we compare the modal profiles computed using this technique to the ones measured on the 3D printed objects. We also demonstrate how the data acquired using these various techniques can be used in a practical context with open-source softwares. Finally, we discuss the results of our experiments and give future directions for this type of work.

2. MATRIX OF SIMPLE RESONATORS

The experiments presented in the following sections of this paper are all based on a matrix of 3D objects implementing simple musical instrument bodies/resonators. These objects are essentially “open boxes” of different shapes and sizes. Figure 1 gives an overview of how the objects are organized in the matrix: the x axis defines the shape of the objects (from circular to square) and the y axis their scale/size. Objects are scaled on this axis which means that

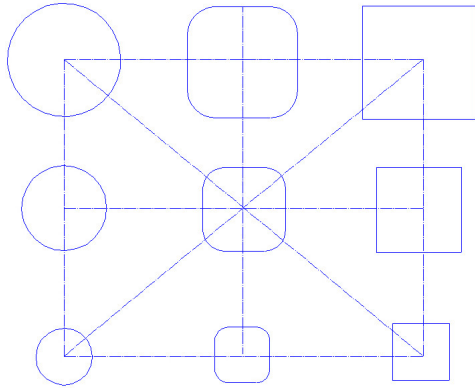
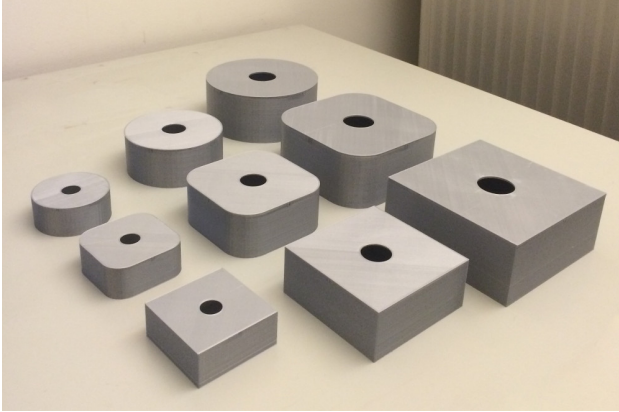


Figure 1. Matrix of 3D printed instrument bodies with their corresponding shape.

Object	Scale	Diam./ Width	Height	Walls	Hole Diam.
Large	2	130	54	4	32
Medium	1.5	81.5	40.5	3	24
Small	1	65	27	2	16

Table 1. Dimensions in millimeters of the objects presented in Figure 1.

all their parameters (including their “wall” thickness) are changed. A scaling factor of 2 was applied to the largest objects of the matrix compared to the smallest ones. Table 1 summarizes the dimension of the objects presented in Figure 1. Note that the size of objects is the same for objects of different shapes.

A generic OpenScad model⁵ was implemented and used to make the model of each object. The nine resonators were 3D printed on a Ultimaker 2 Extended +⁶ which is a Fused Deposition Modeling (FDM) printer. The material used for the prints was PolyLactic Acid (PLA).

This matrix provides an environment for testing different physical parameters in the framework of physical modeling. Therefore, the impact of the scale of the object and of their basic shape on the quality of the models is tested in

⁵The source code of this model is available on the project web-page: <https://ccrma.stanford.edu/~rmichon/3d-printing-modeling>.

⁶<https://ultimaker.com/en/products/ultimaker-2-plus>

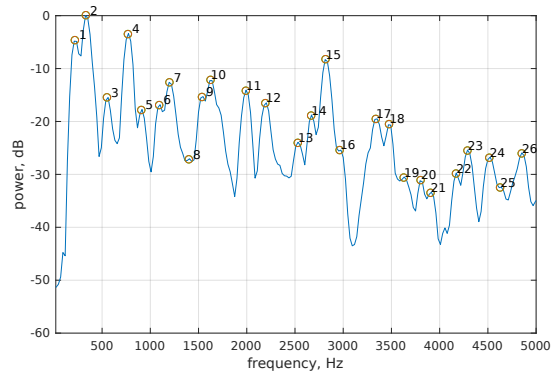


Figure 2. Spectrum and detected modes (numbered and represented by circles) of the large square object of Figure 1.

§4-5. Intermediate elements (e.g., resonators with rounded corners and scale factor 1.5) will also serve as a proof for some of the predictions made by the technique presented in §5.

3. IMPULSE RESPONSE ANALYSIS

The impulse response of each object of Figure 1 was measured in order to compare the acoustics of the printed objects with their modeled version (see §4) and also to make the models presented in §5. Measurements were made in an anechoic chamber using a force hammer and a probe microphone. Impulse responses were measured in different physical locations on the objects but due to the clarity of the recordings, we decided to use the one made at the center of their back plate for experiments presented in this paper.

After deconvolving the signal of the force hammer and the microphone from the overall impulse response, the frequency domain position of the modes and their amplitude was automatically estimated by detecting peaks in the spectrum. Figure 2 gives an example of this process by plotting the spectrum of the impulse response of the large square object with the modes detected by our system. Only modes below 5KHz are plotted as the spectrum of the impulse responses tends to become more chaotic beyond this frequency.

The T60 (resonance duration) of each mode was estimated by tracking their respective decays within spectrograms.

The mode parameters (frequency, gain, and T60) of each object when excited at the center of their back plate were stored in a database to be used in the experiments presented in the following sections. All these operations were done in Matlab.

4. MODELING USING FINITE ELEMENT METHOD

The Finite Element Method is a known technique for modeling the dynamic deformation of an object and synthesizing the sound emitted by the object after an excitation [6].

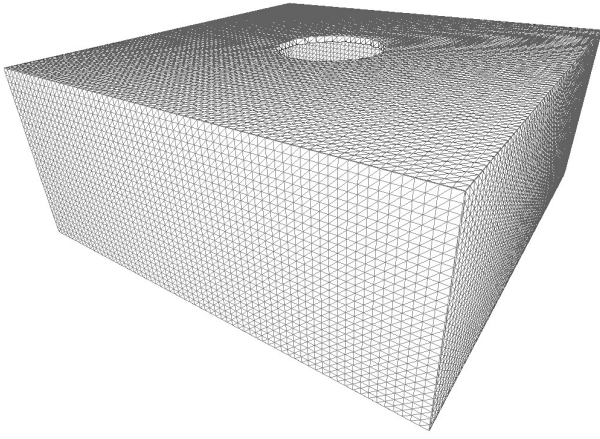


Figure 3. Reworked mesh of the large square instrument body ready for finite element analysis.

It has been successfully used to model the body of string instruments [7] such as the violin [8, 9]. FEM is now commonly employed by modern luthiers as an analysis tool when designing new instruments [10].

In a previous publication, we introduced `mesh2faust` which is an open-source tool [11] to generate modal physical model [12] for the FAUST programming language [13]. `mesh2faust` takes a volumetric mesh of a 3D object as its main argument, carries out a finite element analysis using the Vega FEM Library [14], and generates the corresponding FAUST modal physical model. We wish to keep the tool-chain presented in this paper fully open source to facilitate its use by other members of the community, which is why we decided to use `mesh2faust`.

4.1 Meshing

The optimized meshes produced by OpenScad for each object presented in Figure 1 were re-meshed using MeshLab⁷ in order to create uniform volumetric meshes (see Figure 3). Indeed, even though the stl file generated by OpenScad already hosts a mesh compatible with `mesh2faust`, it is highly optimized and it will not work properly with finite element analysis (see Figure 4). Acousticians using this technique don't necessarily face this issue as they typically draw the optimized mesh directly without using a CAD software. Also, some proprietary (and absurdly expensive) CAD softwares have built-in tools to carry out this task but it is not the case of OpenScad which is open source.

Producing a uniform mesh is challenging as we must strike a balance between a tractable number of faces and a plausible representation of the object. Considering this tradeoff, all square objects have 15980 faces, semi-circular objects have 39964 faces and circular objects have 53980 faces. For reference, computing the modes of a mesh with 50000 faces takes approximately ten minutes in `mesh2faust` on a single core (2.7GHz) Intel i7-2620M CPU.

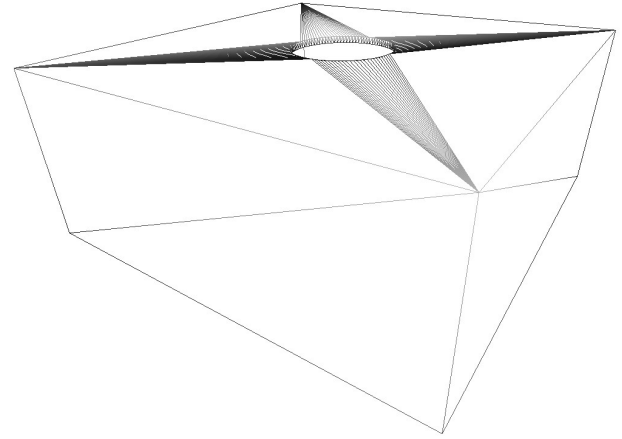


Figure 4. Optimized mesh of the large square instrument body generated by OpenScad.

Object	Young's Modulus (N/m^2)	Poisson Ratio	Density (kg/m^3)
Circular Large	3.3	0.36	1280
Circular Mid	3.5	0.36	1250
Circular Small	3.3	0.36	1250
Semi Circular Large	3.5	0.36	1240
Semi Circular Mid	3.5	0.36	1240
Semi Circular Small	3.3	0.36	1260
Square Large	3.5	0.36	1250
Square Mid	3.5	0.36	1260
Square Small	3.5	0.36	1260

Table 2. Material properties used for the finite element analysis of each object of Figure 1.

4.2 Material Properties

Material properties must be specified in order for `mesh2faust` to carry out finite element analysis. The material used for printing the objects modeled here is PLA (see §1). The standard properties of this type of material (Young's Modulus: $3.5N/m^2$, Poisson's Ratio: 0.36, Density: $1240kg/m^3$) [15] were fine-tuned for each object to best match their impulse response (see Figure 5). Due to inhomogeneous extrusions in fusion deposition modeling, material properties tend to slightly change from one print to another. The material properties used for each object are summarized in Table 2.

4.3 Comparing the FEM Modes to the Impulse Response of the 3D Printed Objects

The mode parameters (i.e., frequency and gain) computed by `mesh2faust` when exciting the models at the center of their back plate are compared to the modes estimated from the impulse response measured at the same location on the 3D printed objects (see §3) in Figure 5.

The results of this experiment are similar for most objects. `mesh2faust` only computes eigen modes, therefore the first few measured modes (generally 1 to 4) are not

⁷<http://www.meshlab.net/>

found as they are probably Helmholtz (“air”) modes [8]. On the other hand, the frequency of the following modes was accurately computed by `mesh2faust`, at least up to 3KHz. Beyond this point, the number of modes yielded by the FEM analysis becomes much higher making it harder to compare FEM and measured modes. We want to emphasize the fact that we had to adjust the material properties used for the analysis independently for each object in order to obtain these results (see §4.2).

5. IMPULSE-RESPONSE-BASED MODULAR MODELING

In a previous publication [16], we investigated the use of mode parameter interpolation as a method to predict the acoustics of simple resonators similar to the one presented in Figure 1. This idea was based on previous works on morphing musical instrument body models [17]. It was also greatly inspired by the famous experiment conducted by Carleen Hutchins in the early 1980s where she compared acoustical differences between scaled violins through labour intensive lutherie, at a time when 3D printing was an emerging and obscure technology [18].

The resonator matrix presented in Figure 1 can be seen as a two dimensional space whose boundaries are defined by the objects at each corner. The idea behind the work presented in this section is to use mode morphing to compute the modal profile of any object within the boundaries of the matrix. Intermediate objects (e.g., intermediate scale and squares with rounded corners) are used in a first step to verify the accuracy of the system, and then to improve its resolution.

5.1 Modes Pairing and Morphing

The modes of each object of Figure 1 were identified using the technique presented in §3. Modes are defined by 3 different parameters: frequency, amplitude, and T60. Mode morphing consists of linearly interpolating mode parameters from one object to another. For this operation to be perceptually realistic, the modes of one object must be paired to the modes of the other [17]. In other words, it is necessary to identify the position in the frequency domain where a mode is translated and vice versa.

While modes generally translate well when a scaling operation is carried out [18], it is not necessarily the case when modifying the shape of an object. Therefore, the modes of the various objects of the matrix of Figure 1 were paired on the y axis (scale) by trying to predict the frequency of the modes of each object by doubling their frequency. Modes were paired only if they translated in a bidirectional way. For example, the modes of the small circular object were paired to the large circular one first by doubling the frequency of the modes of the small one. If their frequencies matched the measured ones, the corresponding modes were associated. A similar operation was then carried out in the other direction (from large to small) by halving the modal frequencies of the large object. If modes matched in both direction, we considered them as

“paired modes” and they were used with our morphing algorithm.

Even though modes are less likely to translate on the x axis of our matrix (shape), we used the same technique to pair modes in this direction. After this operation, some modes were discarded and the number of modes was the same for each object. This algorithm was implemented in a Matlab script that also generated the corresponding FAUST physical model described in §6.

5.2 Comparing the Morphed Modes to the Measured Ones

Figure 6 compares the modes predicted using the technique presented in §5.1 to the modes measured on intermediate objects for all possible object couples at the corners of the matrix (e.g., square - large, square - small, circular - large, and circular - small). Modes beyond 3KHz are not plotted for clarity but similar results were observed for modes between 3KHz and 5KHz.

As expected [18], the modal profile of intermediate objects can be predicted somewhat accurately when morphing is done on the y axis (scale), at least for the first few modes. On the other hand, results are not as convincing when morphing is carried out on the x axis (shape) even though the frequency of some modes did match.

6. APPLICATIONS

The mode parameters of the experiments presented in §4 and §5 were used to implement modal synthesizers [12] compatible with the FAUST Physical Modeling Library (FPML) [19].

The modal synthesizers corresponding to each object presented in Figure 1 using the mode parameters computed by `mesh2faust` in §4 were added to FPML. Indeed, `mesh2faust` is able to generate “ready-to-use” modal models without any additional step. Since `mesh2faust` is currently not able to compute the T60s of the modes (see §4), those were adjusted by hand.

On the other hand, a generic model based on the system described in §5 was implemented from scratch in FAUST. Two of its parameters allow for the control the current x/y position in the matrix of objects by carrying out linear interpolation between mode parameters. The modal data of all the objects of the matrix (including the intermediate one used for proofing in §5) are used in this model to improve its accuracy.

A series of simple physical models of string instruments based on the modal synthesizers described in the previous paragraphs were implemented and integrated to FPML. They’re all based on a template similar to:

```
model = chain(
  guitarNuts :
  steelString(stringL,pluckPosition,
    stringExcitation) :
  guitarBridge :
  inRightWave(bodyExcitation) :
  modularInterpBody(nBodyModes,shape,
    scale) :
```

```
out) ;
```

In FPML, `chain` allows for the creation of bidirectional connections between elements. A generic guitar bridge and nuts were used to terminate a steel string and to couple it to the modal models. Here, `modularInterpBody` corresponds to the generic model based on the system described in §5, `stringExcitation` is an excitation signal to drive the virtual steel string and `bodyExcitation` is an excitation signal to drive the modal model directly.

A series of web-apps were generated using these models and can be played online on the project's webpage.⁸ They constitute a very convenient and interactive way to listen to the results of the experiments presented in this paper.

7. DISCUSSION AND CONCLUSIONS

The combination of 3D printing and physical modeling blurs the boundaries between the physical/acoustical and virtual/digital domains. Digital and traditional lutherie reinforce each other by placing CAD softwares at the intersection of these two worlds.

The initial set of experiments presented in this paper approach these concepts from different angles. §4 uses a standard technique for modeling the objects directly from their graphical representation while §5 introduces a system using a database of measurements made on a series of printed objects within a space with defined boundaries to estimate the acoustics of other objects in that space.

The finite element method used in §4 allowed us to predict the parameters of the modes of the objects presented in §2 with promising accuracy but showed some limitations mostly related to its incapacity to find Helmholtz modes. Moreover, this technique cannot model nonlinearities, which can be quite limiting in various cases. Other techniques such as finite difference schemes [20] can be used to solve these problems but they usually require more computation and they are not always as portable as FEM. Overall, different types of objects (e.g., solids, open resonators, membranes, etc.) require the use of different modeling techniques, and we believe that 3D printing can play an important role in validating these models under highly controlled conditions. Therefore, we plan to conduct similar experiments with different types of objects and modeling techniques in the future.

The technique presented in §5 discards the modeling step and offers promising results, despite some limitations especially when changing the shape of an object rather than its dimensions. Increasing the density of the matrix to provide more data points could help solve this problem. Additionally, machine learning might have a role to play in this by establishing relationship between physical properties under certain conditions and the corresponding modal profile of an object. At scale, computational learning could generalize this problem to much more complex acoustic systems such as rooms (reverberation), etc.

The objects used for our experiments were printed on an entry level FDM printer. More expensive printers are ca-

pable of producing more complex and potentially larger objects. They also offer more consistency on the printed objects which is very important in the framework of our project. On the other hand, printers used by the DIY⁹ community have allowed for widespread access to desktop manufacturing. Indeed this study would not have arisen without such machines and in turn they can play an important role in the replication of such results across small labs.

The matrix of object presented in §2 allowed us to test a limited number of parameters and it would be interesting to carry out similar experiments looking at other parameters. For example, depth is known to play an important role in the acoustical properties of resonators, therefore this parameter would be a good candidate for such experiment.

Combining 3D printing and physical modeling offers new possibilities to luthiers and researchers to prototype new instruments, verify existing models, and to potentially create hybrid instruments combining physical/acoustical and virtual/digital elements [19]. Much work has yet to be done to implement models that will sound exactly the same in both domains. We plan to keep working on this challenge as we advance techniques to bridge virtual and physical acoustics.

8. REFERENCES

- [1] A. Zoran, "The 3d printed flute: Digital fabrication and design of musical instruments," *Journal of New Music Research*, vol. 40, no. 4, pp. 379–387, December 2011.
- [2] S. Summit, "System and method for designing and fabricating string instruments," US Patent, Rock Hill, SC (US), 2014.
- [3] Hovalabs, "Hovalin website," Online, <http://www.hovalabs.com/hova-instruments/hovalin>.
- [4] R. Bader, *Computational Mechanics of the Classical Guitar*. Springer, 2005. [Online]. Available: <http://site.ebrary.com/lib/stanford/reader.action?docID=10145400>
- [5] M. Dabin, T. Narushima, S. T. Beirne, C. H. Ritz, and K. Grady, "3d modelling and printing of microtonal flutes," in *Proceedings of the 16th International Conference on New Interfaces for Musical Expression (NIME-16)*, Brisbane, Australia, 2016.
- [6] C. Bruyns, "Modal synthesis for arbitrarily shaped objects," *Computer Music Journal*, vol. 30, no. 3, pp. 22–37, Autumn 2006.
- [7] N. H. Fletcher and T. D. Rossing, *The Physics of Musical Instruments, 2nd Edition*. Springer Verlag, 1998.
- [8] J. Bretos, C. Santamaria, and J. A. Moral, "Vibrational patterns and frequency responses of the free plates and box of a violin obtained by finite element analysis," *The Journal of the Acoustical Society of America*, vol. 105, no. 3, pp. 1942 – 1950, March 1999.

⁸ <https://ccrma.stanford.edu/~rmichon/3d-printing-modeling>

⁹ Do It Yourself

- [9] C. E. Gough, “A violin shell model: Vibrational modes and acoustics,” *The Journal of the Acoustical Society of America*, vol. 137, no. 3, pp. 1210 – 1225, March 2015.
- [10] R. Bader, J. Richter, M. Mnster, and F. Pfeifle, *Digital Guitar Workshop Manual*, Hamburg University, 2014.
- [11] R. Michon, S. R. Martin, and J. O. Smith, “Mesh2Faust: a modal physical model generator for the Faust programming language application to bell modeling,” in *Proceedings of the International Computer Music Conference (ICMC-17)*, Shanghai, China, October 2017.
- [12] J.-M. Adrien, “The missing link: Modal synthesis,” in *Representations of Musical Signals*. Cambridge, USA: MIT Press, 1991, ch. The Missing Link: Modal Synthesis, pp. 269–298.
- [13] Y. Orlarey, S. Letz, and D. Fober, *New Computational Paradigms for Computer Music*. Paris, France: De-latour, 2009, ch. “Faust: an Efficient Functional Approach to DSP Programming”.
- [14] S. Fun Shing, D. Schroeder, and J. Barbi, “Vega: Non-linear fem deformable object simulator,” *Computer Graphics Forum*, vol. 32, no. 1, pp. 36–48, February 2013.
- [15] J. Thores, J. Cotelo, J. Karl, and A. P. Gordon, “Mechanical property optimization of fdm pla in shear with multiple objectives,” *JOM*, vol. 67, no. 5, 2015.
- [16] R. Michon and J. Granzow, “Predicting the acoustical properties of 3d printed resonators using a matrix of impulse responses and mode interpolation,” *Journal of the Acoustical Society of America*, vol. 139, no. 4, 2016.
- [17] H. Penttinen, M. Karjalainen, and A. Hrm, “Morphing instrument body models,” in *Proceedings of the COST G-6 Conference on Digital Audio Effects*, Limerick, Ireland, December 2001.
- [18] C. Hutchins, “The acoustics of violin plates,” *Scientific American*, vol. 245, no. 4, pp. 170–187, 1981.
- [19] R. Michon, J. O. Smith, M. Wright, C. Chafe, J. Granzow, and G. Wang, “Mobile music, sensors, physical modeling, and digital fabrication: Articulating the augmented mobile instrument,” *Applied Sciences*, vol. 7, no. 12, p. 1311, 2017.
- [20] S. Bilbao, *Numerical Sound Synthesis: Finite Difference Schemes and Simulation in Musical Acoustics*. Chichester, UK: John Wiley and Sons, 2009.

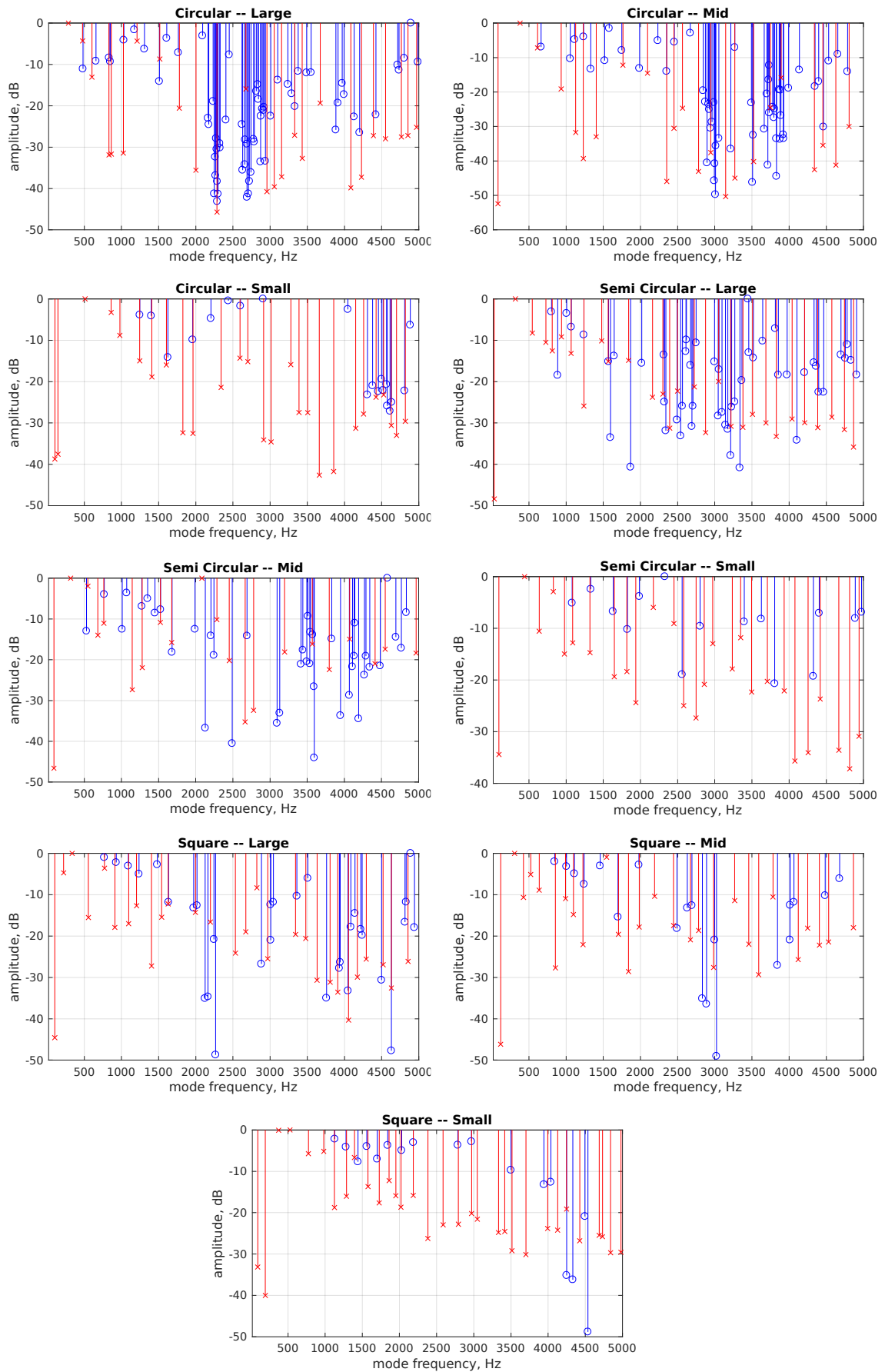


Figure 5. FEM modes computed with `mesh2faust` (in blue and terminated with circles) versus modes measured on the 3D printed objects (in red and terminated with crosses).

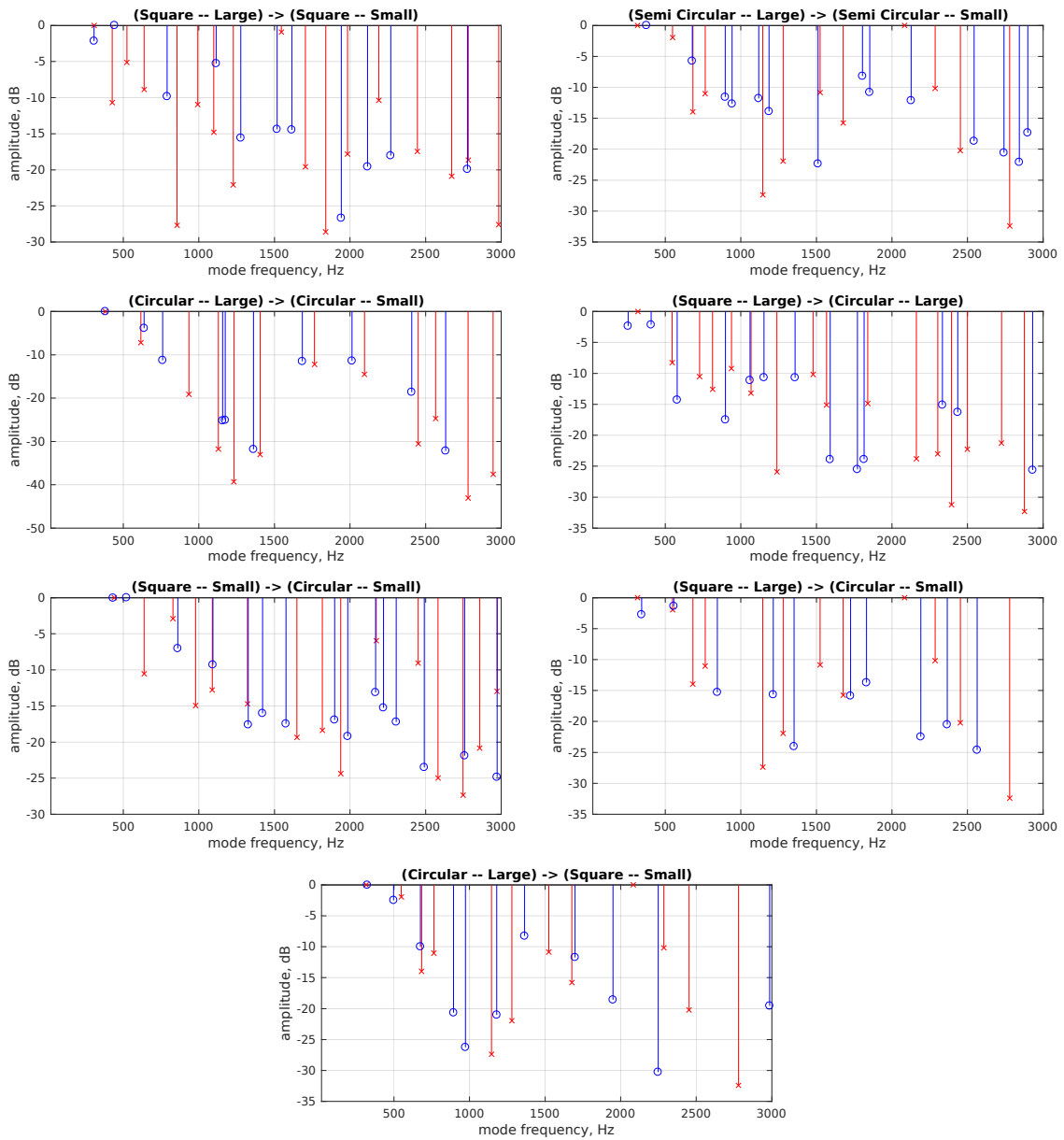


Figure 6. Interpolated modes (in blue and terminated with circles) versus modes measured on the 3D printed objects (in red terminated with crosses) for all possible combinations leading to intermediate objects.